

Modulated mixing and frontogenesis in shallow seas and estuaries

P. F. LINDEN* and J. E. SIMPSON*

(Received 15 May 1987; in revised form 15 January 1988; accepted 16 January 1988)

Abstract—This paper describes some laboratory experiments on the circulation produced in a fluid containing a horizontal density gradient in the presence of environmental turbulence whose level varies periodically with time. The experiments are intended to model the effects of turbulence generated by tidal flow in a shallow sea or estuary. At times of high tidal flow the water column is vertically mixed and the baroclinically driven circulation is weak. At low turbulence levels the baroclinic circulation accelerates and the water column stratifies. The longitudinal flux of density is measured and an effective longitudinal dispersion coefficient K is calculated. The value of K increases with the horizontal density gradient and also with the period of the turbulence modulation. This latter increase is a result of the enhanced flux driven by the baroclinic circulation at low turbulence levels. The results of these experiments are compared with some recent measurements of episodic mixing events in Liverpool Bay, U.K., Spencer Gulf, South Australia, and the Columbia River Estuary, U.S.A.

1. INTRODUCTION

STIRRING by tidally driven flows is an intrinsic aspect of the circulation in shallow seas and in estuaries. Turbulence is generated by bottom stresses and this turbulent kinetic energy is available to mix the water column. The opposing tendency for the water column to stratify arises from two distinct processes. The first is a baroclinic circulation, driven by a horizontal density gradient which causes dense water to flow underneath fresher, less dense water. In estuaries the horizontal density gradient is associated with the variation of salinity along the estuary. The ability of the tidal flow to mix this stratification and maintain vertically homogeneous conditions increases with the strength of the tide and is most effective in shallow estuaries.

The nature of the flow, and the resulting along-estuary flux of salt and other contaminants is quite different when the estuary is stratified compared with when it is mixed. In general, the stratified estuary, with its lower turbulence levels, has paradoxically a more rapid along-estuary transfer driven by the baroclinic circulation. The importance of these different flow regimes have been known for many years and the earliest classification of estuaries as well-mixed, partially mixed or stratified was made by SIMMONS (1955), on the basis of ratio of the river flow during a tidal cycle compared with the tidal prism. HANSEN and RATTRAY (1966) devised a two parameter description using properties $\Delta S_0/S$, the ratio of the vertical salinity difference to the sectional mean salinity, and U_s/U_t , the ratio of the mean tidal surface velocity to the freshwater flow. Both the parameters in the Hansen and Rattray prescription are averages over tidal cycles, and as recently pointed out by JAY and SMITH (1988) these averages can remove the major ingredient of the estuarine flow, viz. the tides themselves.

* Department of Applied Mathematics and Theoretical Physics, University of Cambridge, Silver Street, Cambridge CB3 9EW, U.K.

JAY and SMITH (1988) suggest an alternative means of classifying an estuary based on bulk Froude numbers of the barotropic tidal flow and of the baroclinic circulation associated with the horizontal density stratification. They also show that the stratification in an estuary can vary both during an individual tidal cycle and over the springs – neaps cycle of the tide. Data measured in the Columbia River Estuary show that, at the end of the flood tide during springs, an almost uniform horizontal density gradient is found over 30 km from the mouth, with very weak vertical gradients. At the same phase of the tide on the neaps a strong front is formed on the bottom of the estuary about 25 km from the mouth and a significant vertical density gradient has been established. Similar differences exist at the end of the ebb, but they are not so pronounced (see Figs 1 and 2 of their paper). JAY and SMITH (1988) propose that the transition from stratified to vertically mixed is associated with shear instability and is characterized by a critical internal Froude number.

The second stratifying process more associated with shallow seas, results from solar radiation during the spring and summer. This leads to a layer of warm, less dense water being produced near the surface and the turbulence generated by the tides mixes this warm water downwards. If the surface heat flux is too large, or the turbulence insufficiently strong, a stable stratification will develop. Once this occurs the stratification inhibits further mixing and the system has positive feedback (HOPFINGER and LINDEN, 1982). Horizontal variations in stratification can occur as a result of variations in the fluid depth or the strength of the tidal flow. Regions where the turbulence levels are high may be vertically mixed while adjacent areas with lower turbulence levels are stratified. The transition zones between the stratified and mixed regions are observed to be characterized by sharp density gradients or fronts. Since the surface heating is relatively uniform in space the criterion for the transition zone has been expressed in terms of the parameter U^3/H , where U is the mean tidal velocity and H is the fluid depth (SIMPSON and HUNTER, 1974). More recently alternative expressions have been proposed and a good discussion and comparison with observations can be found in LODER and GREENBERG (1986).

The details of the appropriate criterion, while important, are not of direct relevance to the present discussion. The point emphasized here is that in the vicinity of the “tidally-stirred” front the buoyancy forces associated with the horizontal density gradients drive a baroclinic cross-frontal circulation which tends to stratify the mixed region. This circulation is greater at times of low tidal stirring and variations in the position of tidal fronts have been correlated with the spring–neaps cycle of the tides. It is also possible that variations may occur during a single tidal cycle and observations of the front in Liverpool Bay (CZITROM, 1986) show evidence of this.

Another example of the temporal adjustment of a stratified shallow region has been recently described by NUNES and LENNON (1987). They describe the motion of isopycnal surfaces in Spencer Gulf, South Australia during a period when tidal motion was very weak. Their observations are discussed in detail in Section 5 after some relevant laboratory experiments are described in Sections 2 and 3. The experiments model the effects of periodically varying turbulence, such as that produced by a tidal flow over a number of tidal cycles, on a fluid containing a horizontal density gradient. At the times when the turbulence level is low, the baroclinic circulation drives a horizontal density flux which is, in general, greater than at times when the turbulence level is high and vertically mixed conditions prevail. Measurements of the horizontal flux are made and these are

related to the natural timescales of the flow. Calculations of the baroclinic flow are presented in Section 4. The paper ends with some concluding remarks in Section 6.

2. EXPERIMENTS

The experiments were designed to investigate the response of a fluid containing a horizontal density gradient to environmental turbulence whose amplitude varies periodically in time. The turbulence was produced by bubbling air through a manifold on the bottom of a tank measuring 180 cm long, 10 cm wide and with a working depth of 15 cm. The turbulent velocities are a function of the air flow rate per unit area and turbulence scales are comparable with the size of the bubbles. A square wave, “on-off”, air flow rate was used with period τ as shown in Fig. 1. The horizontal density gradient was initially established by “lock-exchange” in which a barrier separating two regions of different density is withdrawn as shown in Fig. 2. More details of the apparatus and the turbulence are given in LINDEN and SIMPSON (1986) where this technique was used for studying the influence of environmental turbulence on gravity currents.

Observations of the motion were made with shadowgraph and by adding small quantities of food dye to regions of the flow. These observations are discussed in the next section. The main results from this paper are measurements of the horizontal flux of density along the tank. The method used to determine this flux has been discussed by LINDEN and SIMPSON (1986) and so only a brief description will be given here and the reader is referred to our earlier paper for more details.

The density differences in the tank were produced by dissolving NaCl in the water, and the density was measured using a conductivity probe or by withdrawing samples and measuring the refractive index of the solution. The density was measured at mid depth at

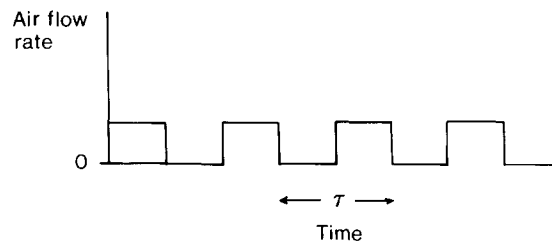


Fig. 1. The air flow rate as a function of time.

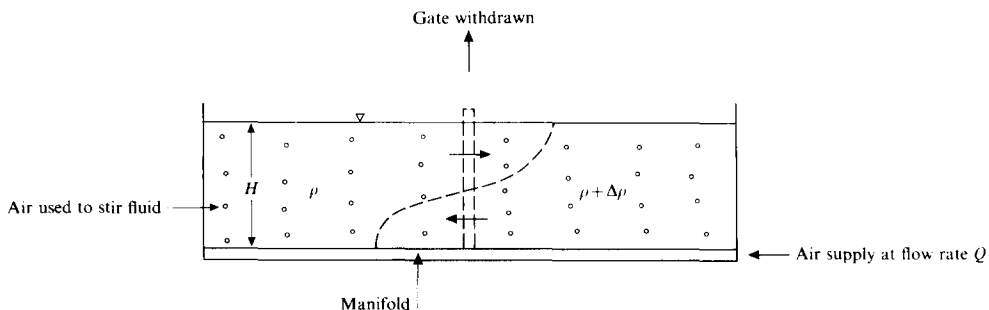


Fig. 2. A sketch of the experimental apparatus.

5 cm from each end of the tank at discrete times during each experiment. The measurements were taken during periods in which the bubbles were turned on so that the water column was well mixed and the density measurements are vertical averages. As discussed in LINDEN and SIMPSON (1986), if the transport of salt along the tank can be described as a Fickian process with a longitudinal dispersion coefficient, K , then plots of

$$-\ln\left\{1 - 2 \frac{S(-\frac{1}{2}L, t)}{S_0}\right\}$$

vs time, where $S(-\frac{1}{2}L, t)$ is the salinity at one end of the tank and S_0 is the initial salinity difference on the two sides of the barrier, yield straight lines with slope proportional to K . An example of a plot from one experiment is shown in Fig. 3. Over sections of the data, which cover several turbulence periods τ , the observations can be represented as straight lines as drawn in the figure. The decreasing slope of the line segments with time is due to the decreasing baroclinic transport as the density difference between the ends of the tank diminishes.

In the measurements discussed below the values of K determined from each line segment are determined. These are plotted in the following way. In order to estimate the strength of the baroclinic driving, a baroclinic parameter $B = g\alpha H^2/q^2$ is evaluated. The baroclinic effects are described by the horizontal density gradient $\alpha = |(1/\rho)\partial\rho/\partial x|$ and g is the acceleration due to gravity. The fluid depth is H and q is an r.m.s. turbulence intensity associated with the bubbles. The value of q is determined from the *mean* air flow rate (i.e. one-half the "on" value) for a given experiment as described in LINDEN and SIMPSON (1986). As K increases with the baroclinic driving $K = K(B)$, and we plot values normalized by $K(0)$, which is the dispersion coefficient due to the bubbles alone ($\alpha = 0$). The values of $K(0)$ were determined by measurements of passive dispersion as discussed in LINDEN and SIMPSON (1986). As for B , the value of $K(0)$ appropriate to the *mean* air flow rate is used.

The experimental parameters are shown in Table 1.

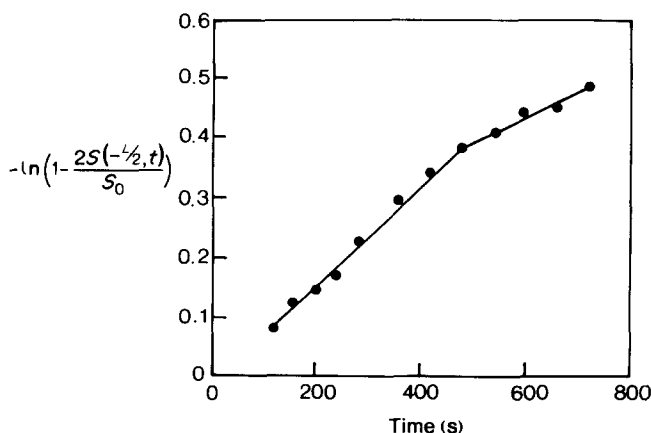


Fig. 3. A plot of $-\ln\{1 - 2S(-1/2L, t)/S_0\}$ against time t for a run with periodic turbulence with period $\tau = 20$ s. The straight lines are fitted to the data by eye.

Table 1. *The experimental parameters*

Exp. No.	τ (s)	H (cm)	$g\alpha$ ($\times 10^{-2} \text{ s}^{-2}$)	K ($\text{cm}^2 \text{ s}^{-1}$)	B
1	20	12	8.8	12.5	0.35
2	20	12	4.1	5.1	0.61
3	40	12	2.4	10.0	0.09
4	40	12	6.5	25.0	0.35
5	40	14	2.4	9.0	0.13
6	40	14	1.8	4.9	0.10
7	40	12	9.1	16.0	0.37
8	40	12	5.3	9.7	0.21
9	40	12	3.5	5.0	0.14
10	20	12	8.2	3.6	0.32
11	20	12	5.3	2.7	0.21
12	20	12	2.9	1.4	0.13
13	10	12	8.2	10.1	0.32
14	10	12	4.1	7.0	0.16

3. EXPERIMENTAL RESULTS

The qualitative nature of the flow is very different during the on and off periods of the bubbles. When the bubbles are turned off the turbulence begins to decay. Decay times are of the order of l/q , where l is the length scale of the turbulent eddies. Bubbles generate turbulence of a scale comparable to their diameter (5 mm) and typical values of q are 10 mm s^{-1} giving decay times of about 1 s. Accurate measurements were not made but the turbulence level did appear to diminish significantly within 1 or 2 s. Almost immediately the bubbles were turned off, the baroclinic circulation was observed to accelerate. Dense fluid was advected underneath the less dense fluid by this circulation and a vertical density gradient developed. In addition, mass was transported horizontally by the flow.

If the time before the bubbles are turned back on is long enough, non-uniformities in the horizontal density gradient associated with the ends of the tank can cause a front to form (LINDEN and SIMPSON, 1986). An example of this is shown in Fig. 4. The ensuing motion takes the form of a gravity current and further increases the vertical density gradient in the mid-depth plane so that a two-layer counterflow is established. This flow is extremely efficient at horizontal transport of mass.

When the turbulence is re-established, which occurs almost immediately after the bubbles are turned on, it mixes the vertical stratification and reduces the baroclinic circulation. In these experiments the turbulence was always sufficiently energetic to completely destroy the vertical stratification. A sequence of photographs showing the destruction of the vertical stratification is shown in Fig. 5. The motion of dye patches showed that the baroclinic circulation is much less during the turbulent periods.

The flow within the tank consists of two phases. When the environment is stirred by the turbulence, vertical density gradients are weak. The horizontal density gradient in the tank drives a baroclinic circulation which is balanced by the turbulent dissipation. The longitudinal transport of density is produced by a combination of turbulent dispersion and the baroclinic circulation. When the environment is non-turbulent the dissipation is much reduced. The horizontal density gradient then accelerates the baroclinic circulation which then provides a longitudinal flux of mass.

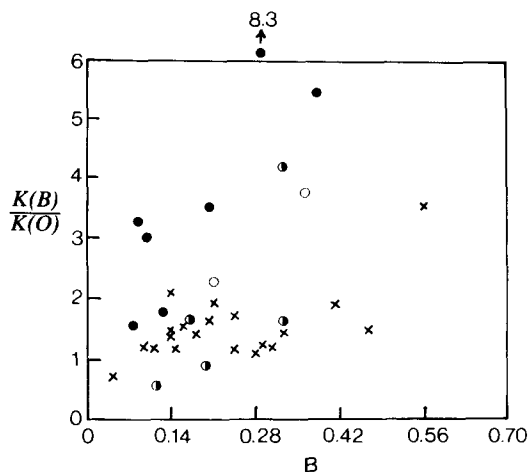


Fig. 6. The longitudinal dispersion coefficient $K(B)$ normalized by $K(0)$, the value due to the bubbles alone, plotted against the baroclinic parameter B . The crosses correspond to flows in which the turbulence level is constant in time. The other points correspond to modulated turbulence with period τ : \circ , $\tau = 10$ s; \odot , $\tau = 20$ s; \bullet , $\tau = 40$ s.

At the values of turbulence intensity used in these experiments the baroclinic circulation was more efficient at transporting density along the tank than was the turbulence. Thus the more time that the baroclinic circulation was allowed to develop in between the turbulent periods, the greater was the horizontal flux of density. This result is shown in Fig. 6 which plots the longitudinal dispersion coefficient $K(B)$, normalized by $K(0)$, against the baroclinic parameter B as discussed in Section 2. The data indicated by crosses are values measured when the turbulence level remains constant in time (i.e. the bubbles remain on throughout the experiments). Those points indicated by circles are data from the periodic turbulent flows and the different shading of each circle indicates the period τ of the oscillation (see Fig. 1). There is considerable scatter in the data which reflects the imprecise nature of these measurements, and error bars are not provided since they are impossible to estimate on any reliable basis. The uncertainty in the data is probably best estimated by the scatter in the data indicated by crosses.

Nevertheless, the trend in the data is clear. For a given B , as the period τ of the intermittency of the turbulence increases, the value of $K(B)/K(0)$ increases. The increase in the dispersion coefficient with τ results from the enhanced transport during the non-turbulent phases as the baroclinic circulation accelerates. The *relative* increase $K(B)/K(0)$ also increases with increasing B , again as a result of the increased baroclinic effects at large B corresponding to larger *horizontal* density gradients.

The data presented in this figure are the main results of these experiments. A model to account for these observations is presented in the next section.

4. THE BAROCLINIC CIRCULATION

It is observed that in our experiments the baroclinic circulation is very weak during the non-turbulent phases. Previous measurements (LINDEN and SIMPSON, 1986) show that during the turbulent phase the fluid is vertically mixed and, with the exception of regions

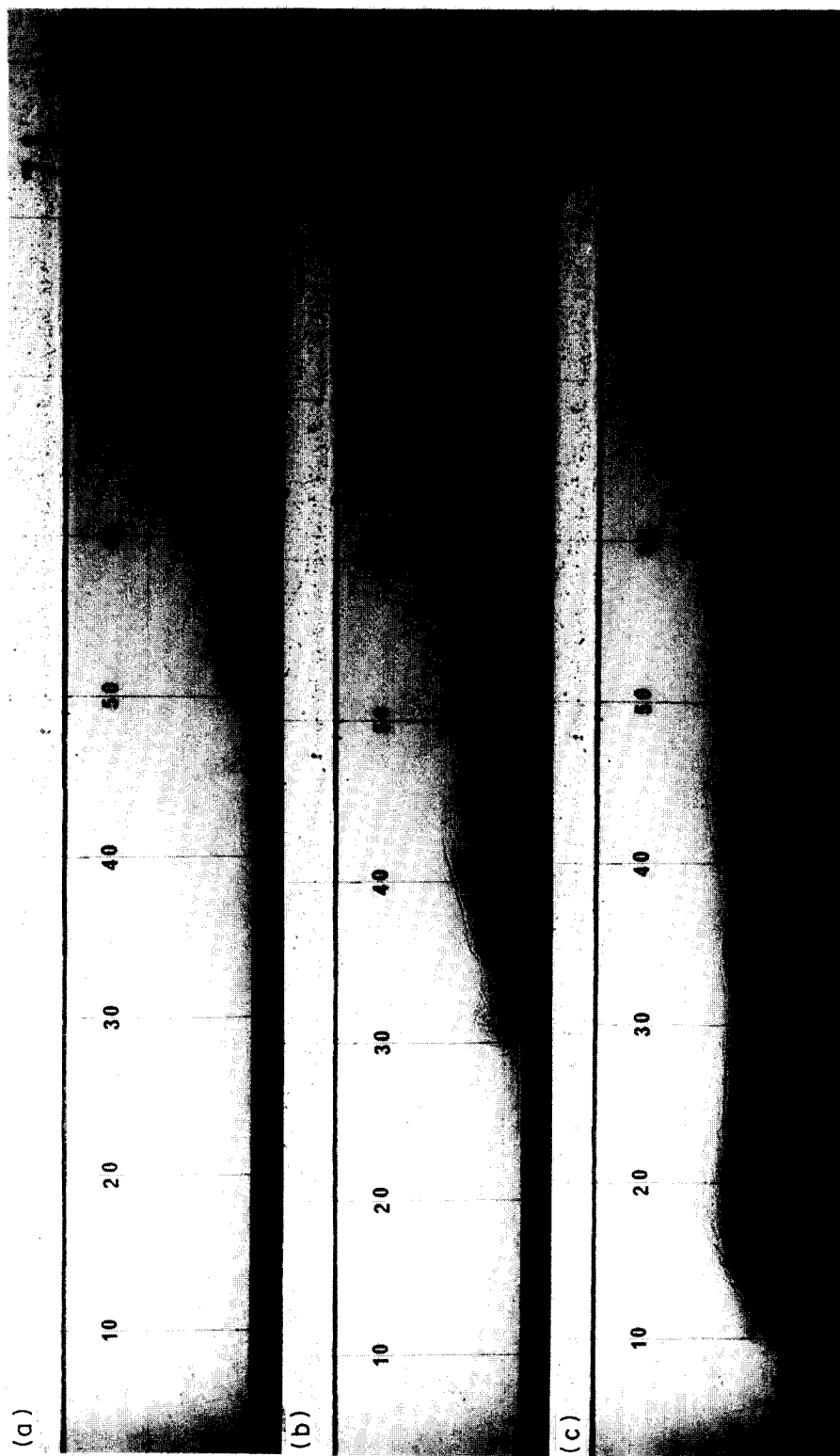


Fig. 4. Frontogenesis, the formation of a gravity current, after the turbulence ceases. In this example the fluid was vertically mixed and the buoyancy difference between the ends of the tank when the bubbles were turned off was $g' = 0.05 \text{ m s}^{-2}$ and the depth $H = 0.12 \text{ m}$. The photographs were taken at (a) 8.9 s, (b) 10.8 s and (c) 17.4 s after the bubbling ceased.



Fig. 5. The evolution of the density driven circulation in the presence of environmental turbulence. The initial buoyancy difference $g' = 0.2 \text{ m s}^{-2}$ and $H = 0.12 \text{ m}$. The photographs were taken at (a) 4.2 s, (b) 8.9 s and (c) 12.7 s after the removal of the gate.

near the end of the tank, the density varies linearly with horizontal position. We will calculate the baroclinic circulation by supposing, therefore, that at the beginning of the non-turbulent phase the fluid is at rest and that the density is a linear function of the horizontal coordinate x only. We ignore any time taken for the turbulence to decay.

The initial conditions can be expressed as

$$\mathbf{u} = (u, w) = (0, 0) \quad \rho = \bar{\rho}(1 - \alpha x), \quad (1)$$

where $\alpha > 0$ is a constant. The fluid density increases to the left ($x < 0$) and we restrict attention to a two-dimensional motion in the $x - z$ plane, where z is the vertical coordinate. The equations governing the Boussinesq, inviscid flow under the assumption that $w = 0$ are

$$\begin{aligned} \bar{\rho} u_t &= -p_x, & g\rho &= -p_z, \\ \rho_t &= -u\rho_x, & u_x &= 0. \end{aligned} \quad (2)$$

This motion has been discussed by SIMPSON and LINDEN (1988) and so we merely draw attention to the features relevant here. Elimination of the pressure p and use of mass continuity shows that

$$\rho_{xx} = 0, \quad (3)$$

and so the horizontal density gradient remains constant at its original value $-\alpha\bar{\rho}$ throughout the motion. The solution is

$$u = -g\alpha zt, \quad \rho = \bar{\rho}(1 - \alpha x) - \frac{1}{2} g\bar{\rho}\alpha^2 zt^2. \quad (4)$$

A uniform vertical shear flow is established which accelerates at constant rate. The isopycnals remain straight and rotate towards the horizontal with

$$\tan \theta = \frac{1}{2} g\alpha t^2, \quad (5)$$

where θ is the angle of an isopycnal to the vertical. A sketch of the flow is shown in Fig. 7. The vertical density gradient increases as the flow accelerates with

$$\rho_z = \frac{1}{2} g\bar{\rho}\alpha t^2, \quad (6)$$

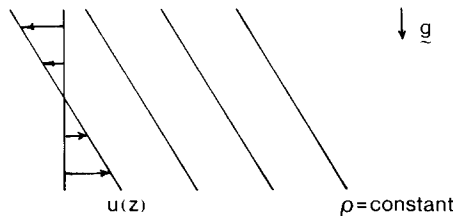


Fig. 7. A sketch of the shear flow and the isopycnal displacement generated by the adjustment under gravity of a fluid containing a uniform horizontal density gradient. Note that isopycnals that are initially vertical remain straight during the motion and rotate towards the horizontal. The horizontal density gradient remains constant with time.

and the gradient Richardson number $Ri = g\rho_z/\bar{\rho}u_z^2 = 1/2$ is constant in space and time. Thus the baroclinic circulation is expected to remain stable to small disturbances.

The horizontal flux F of density is given by

$$\begin{aligned} F &= -2 \int_0^{H/2} u \rho_x dz, \\ &= -\frac{1}{4} g \bar{\rho} \alpha^2 H^2 t, \end{aligned} \quad (7)$$

where H is the depth of the flow (in this case the tank depth). The longitudinal dispersion coefficient $K_b(B)$ associated with the baroclinic flow is given by

$$\begin{aligned} K_b(B) &= F/\rho_x, \\ &= \frac{1}{4} g \alpha H^2 t. \end{aligned} \quad (8)$$

The value of K_b is given by the mean value associated with the baroclinic circulation over the time $t = \tau/2$, i.e.

$$K_b = \frac{1}{16} g \alpha H^2 \tau. \quad (9)$$

The longitudinal dispersion coefficient K_b is predicted to increase linearly with the period τ of the turbulence modulation and in proportion to the horizontal density gradient. Measurements of the dispersion coefficient K are plotted against $1/16 g \alpha H^2 \tau$ in Fig. 8. These data are the same as those shown in Fig. 6 and, as commented in connection with that figure, the scatter is large. The solid line is the predicted value given by (9). The trend in the data is consistent with the prediction although the measured values of K_b are, in general, less than the estimate from the baroclinic circulation. Part of this discrepancy results from the fact that in the experiments the turbulence does not decay instantaneously, and so the baroclinic circulation does not develop immediately the bubbles cease.

In order to evaluate the dispersion coefficient in an oscillating turbulent field with period τ as shown in Fig. 1 we estimate the mean dispersion coefficient to be given by

$$K = \frac{1}{2} \left[K_t + K_b \right], \quad (10)$$

where K_t is the value of $K(B)$ for a continuously turbulent environment and is given by the crosses in Fig. 6. These data are represented approximately by (LINDEN and SIMPSON, 1986)

$$\frac{K_t(B)}{K_t(0)} = 1 + 0.22 B^{1/2}. \quad (11)$$

Substituting (9) and (11) into (10) we find

$$\frac{K(B)}{K_t(0)} = \frac{1}{2} \left[1 + 0.22 B^{1/2} + \frac{1}{16} \frac{g \alpha H^2 \tau}{K_t(0)} \right]. \quad (12)$$

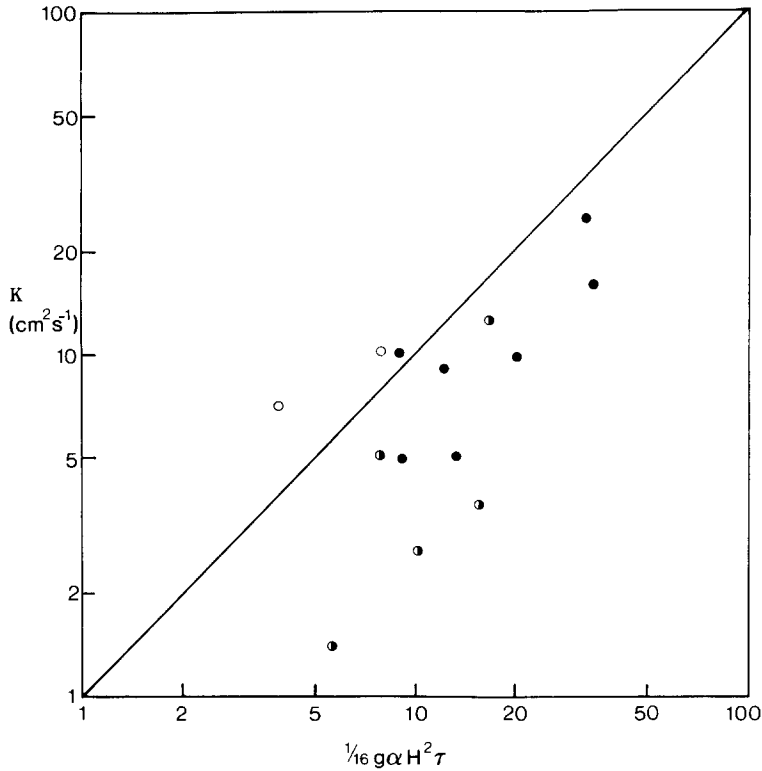


Fig. 8. The longitudinal dispersion coefficient K plotted against $1/16g\alpha H^2\tau$. The symbols are defined in the text and the points on the figure for different values of τ are annotated as in Fig. 6. The solid line is the theoretical result (9).

The effects of baroclinicity on the longitudinal dispersion are measured by the second and third terms on the right-hand side of (12). The baroclinic circulation in the non-turbulent phase compared with that in the turbulent phase is given by the ratio

$$A = \frac{1}{16}g\alpha H^2\tau/0.22B^{1/2}K_t(0) \quad (13)$$

In a flowing stream, $K_t(0) \sim qH$ and so $B = g\alpha H^4/K^2(0)$. Substituting these values into (13) we find

$$A \sim (g\alpha)^{1/2}\tau. \quad (14)$$

This relates the strength of the baroclinic circulation to the ratio of the timescale of the gravitational response $(g\alpha)^{-1/2}$ to the oscillation period τ of the turbulence level. A plot of $K(B)/K(0)$ against this ratio is shown in Fig. 9 and we observe that the effective dispersion coefficient increases as the turbulence level period increases.

The ratio R of the baroclinic density flux to the turbulent density flux is given by

$$R = \frac{1}{16}g\alpha H^2\tau/K_t(0) \sim \frac{1}{16}B^{1/2}(g\alpha)^{1/2}\tau. \quad (15)$$

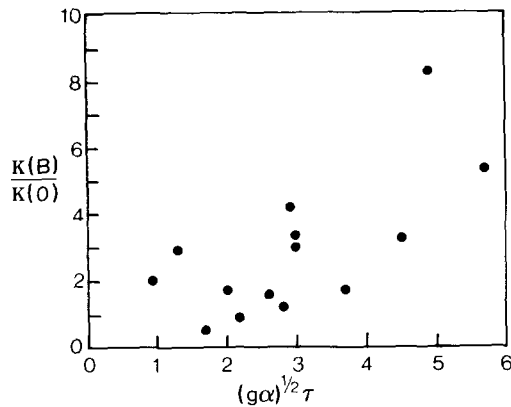


Fig. 9. The normalized longitudinal dispersion coefficient $K(B)/K(0)$ plotted against the dimensionless time scale $\tau(g\alpha)^{1/2}$.

Again this increases with $(g\alpha)^{1/2}\tau$ but is also an increasing function of B . Hence at very high turbulence levels, when $B \rightarrow 0$, R is reduced and the baroclinic flux plays only a small part in the overall transport of density. This region of parameter space was not covered by the experiments described in Section 3, and this behaviour is not found in the data.

5. COMPARISONS WITH FIELD OBSERVATIONS

The experiments described above allow the baroclinic contribution to the longitudinal density flux to be estimated in a situation where the background turbulence level varies in time. Previous experiments described in SIMPSON and LINDEN (1988) showed that in a fluid containing a non-uniform horizontal density gradient a front could be formed at the position of maximum curvature in the horizontal density variation. Those earlier experiments also provided estimates of the timescale for frontogenesis. The results of these and the present experiments will now be extrapolated to oceanic scales and compared with recent field observations. Three cases will be examined in some detail: a tidally stirred front in Liverpool Bay, U.K., an estuarine configuration in Spencer Gulf, South Australia and the Columbia River Estuary, U.S.A.

Liverpool Bay

A field programme was mounted in May 1985 to examine the structure of the Liverpool Bay Front, a feature which separates a well-mixed region to the west from a stratified region closer inshore to the east. The surface water nearer the coast is supplied with fresh water from the rivers Dee and Mersey producing a vertical stratification which is strongest in the winter and spring when the river run-off is greatest (CZITROM, 1986). Details of the field programme are given in SIMPSON *et al.* (1988), and the reader is referred to those papers for further information. We shall concentrate here on the aspects of these observations related to the present experiments. A map of the area showing surface contours of σ_t is shown in Fig. 10a. During the observation period no pronounced front was observed, although a strong horizontal density gradient is present. Figure 10b shows the results of a CTD survey along transect T1 of

Fig. 10a taken near high water on 6/7 May 1985. The water column is well mixed in the vertical, and from the spacing of the contours it is clear that the horizontal density gradient is larger in the eastern part of the transect. SIMPSON *et al.* (1988) fit an expression of the form $S = S_0 + ax + bx^2$ to the salinity measured on 6/7 May 1985. The distance x is measured eastwards from the mooring at A in Fig. 10a, and they obtain the values $a = -4.3 \times 10^{-2}\text{‰ km}^{-1}$ and $b = -8.9 \times 10^{-4}\text{‰ km}^{-1}$. We shall return to the implications of these values below.

The tidal flow is predominantly east-west with a tidal excursion of approximately 10 km. There is considerable vertical shear in the tidal flow with horizontal displacements on the flood and ebb being about 13 km near the surface and 9 km near the bottom. This difference is shown in Fig. 11a where the eastward displacement of the top (solid curve)

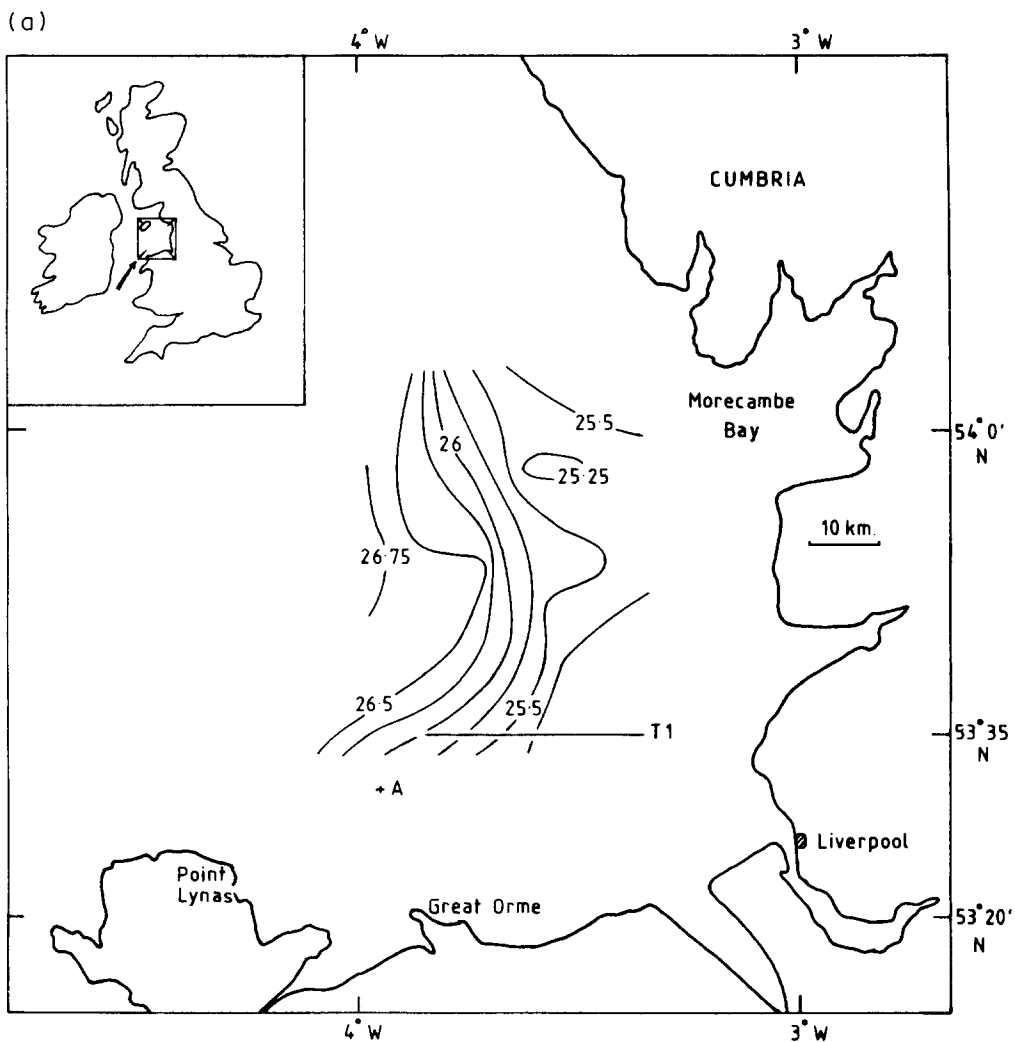


Fig. 10a.

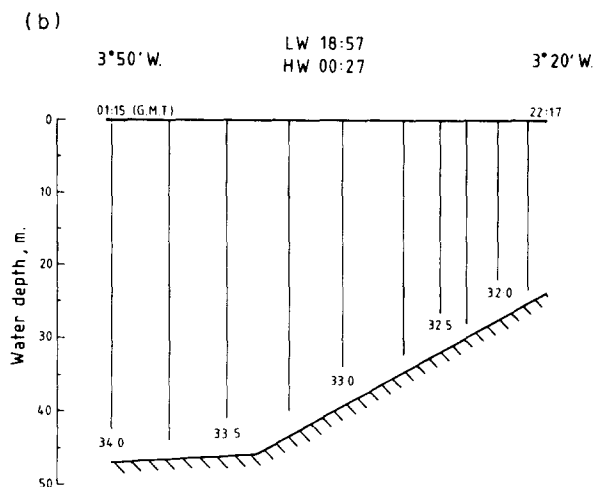


Fig. 10. (a) A map of the Liverpool Bay radar experiment. The ship-based CTD survey was performed along transect TI. (b) Values of the salinity measured along transect TI near high water on 6/7 May 1985. Note that the water column is mixed vertically and the magnitude of the horizontal salinity gradient increases towards the east.

and top-bottom (broken curve) current meters on mooring A, which have a vertical separation of about 30 m, are shown. The lower panel of Fig. 11b shows the bottom-top salinity difference during the period 13–19 May 1985. The size of the salinity difference gives a measure of the vertical stratification of the water column. There is a large variation in the vertical salinity difference which is in phase with the tidal flow. Vertical salinity differences of up to 1‰ develop on the ebb tide and correspond with the maximum westward displacement of the tide. On the flood tide vertically mixed conditions prevail.

Provided regions of mixed and stratified water are not simply advected past the mooring at A on every tide, and transects such as that shown in Fig. 10b suggest they are not, these observations show a temporal change from mixed to stratified conditions on each tide. SIMPSON *et al.* (1988) describe what appears to be the heart of the matter. They imagine the density field to be “frozen” and advected by the tidal flow. The larger tidal excursion near the surface means that on the flood denser water is advected over the top of less dense water and convective instability results, thereby mixing the water column. On the ebb tide fresher water from inshore is advected over the denser water and a vertical stratification is established. A similar mechanism is identified as the cause for observations of periodic variations in vertical temperature gradients in the East China Sea by BURT *et al.* (1986). By evaluating the relative vertical displacement on the ebb (about 4 km) and using the observed horizontal salinity variation, SIMPSON *et al.* (1988) can account for a vertical salinity difference of about 0.3‰. The observed salinity differences shown in Fig. 11b are almost always considerably larger than this value.

This discrepancy may be accounted for by considering the baroclinic circulation which is established during the period of low tidal flow. From (6) we can estimate the time taken to establish the observed vertical salinity difference. Using the observed values of $H = 30$ m, $\alpha = 1 \times 10^7 \text{ m}^{-1}$, the time t taken for the baroclinic circulation to produce the

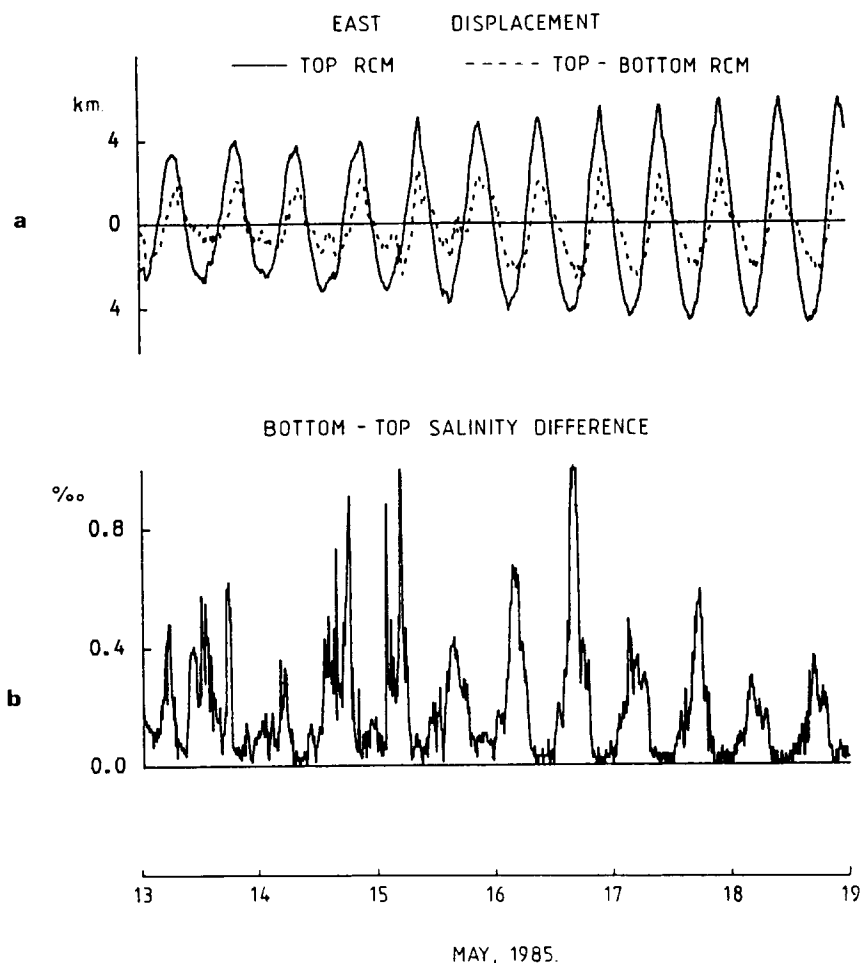


Fig. 11. (a) The solid curve shows the east-west displacement obtained by integrating the top current meter data for the period 13–19 May 1985. The relative (top–bottom) displacement is shown as the broken curve. (b) The lower panel shows the salinity difference (bottom–top) recorded at point A in Fig. 10. Note that the maximum vertical stratification occurs at points of maximum westward displacement of the tide, i.e. at the end of the ebb.

largest observed vertical density difference of 0.7 kg m^{-3} (corresponding to a vertical salinity differences of 1‰) is $t = 4 \text{ h}$. This time is less than the period of ebb tide (7 h) and so this additional baroclinic circulation may account for the observed vertical density differences. It is noticeable in Fig. 11 that the maximum vertical salinity differences occur at the point of maximum ebb displacement when the tidal currents are weakest and the background turbulence is least. At this time the baroclinic circulation should be the most effective at developing a vertical stratification.

SIMPSON and LINDEN (1988) discussed conditions under which frontogenesis occurs in a horizontally stratified fluid. They showed that the tendency to form a front depends on the curvature in the horizontal density profile. LINDEN and SIMPSON (1988) considered a piecewise linear horizontal density profile with horizontal density gradients given by $\rho\alpha_1$

and $\rho\alpha_2$. They found that frontogenesis occurred on a timescale

$$t_c = 4[g(\alpha_1 - \alpha_2)]^{-1/2}. \quad (16)$$

From the sectional data shown in Fig. 10b, we estimate $\alpha_2 = 2\alpha_1 = 1 \times 10^{-7} \text{ m}^{-1}$, which gives $t_c = 1.5 \text{ h}$. It is expected, therefore, that frontogenesis may occur although the process is inhibited by background turbulence. The form of the stratification ($\rho_x < 0$,

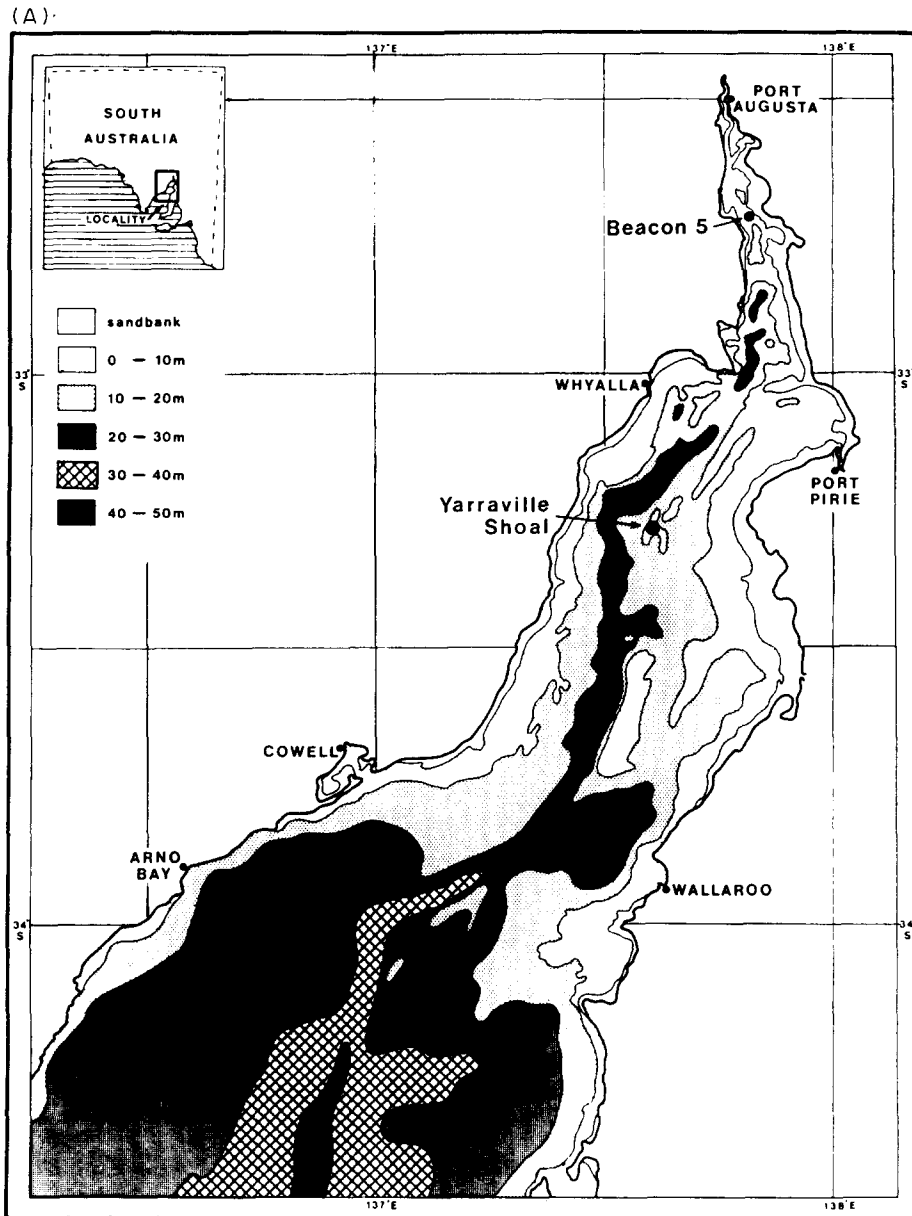


Fig. 12A.

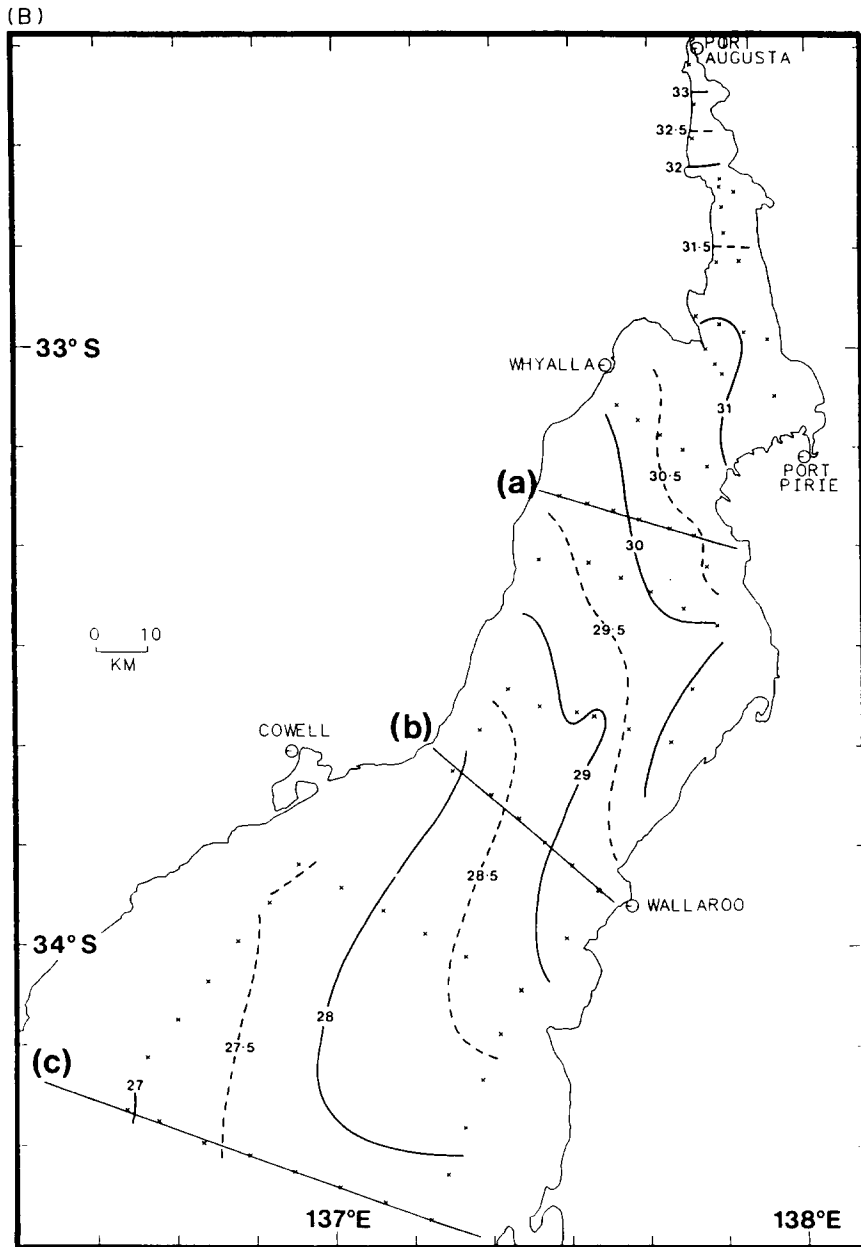


Fig. 12. (A) A map of Spencer Gulf, South Australia, showing the bottom topography. (B) Depth-averaged σ_t (kg m⁻³) in Spencer Gulf during the period 21–23 June 1983. The location of the three vertical sections shown in Fig. 13 are labelled (a), (b) and (c).

$\rho_{xx} < 0$) implies the front should form at the surface and propagate westwards (see SIMPSON and LINDEN, 1988). The lack of any observed surface front suggests that the environmental turbulence is continuing to play a role over a significant part of the ebb tide.

Spencer Gulf

NUNES and LENNON (1987) discuss the gravitationally driven circulation in this shallow bay in South Australia. Figure 12a shows the location and topography of Spencer Gulf. The region is one of high evaporation and the density variations are dominated by the resulting salinity variability. The highest salinities (33‰) are found at the shallow northern end, and the salinity decreases towards the open sea, as shown in Fig. 12b. For this reason it is an example of a negative or inverse estuary (PHILLIPS, 1966).

The interesting feature of Spencer Gulf is the fact that due to an equality in the lunar and solar semidiurnal tidal constituents, there is a loss of semidiurnal tidal currents on a regular 14 day cycle. If the period of low tidal flows coincides with a period of weak winds, then the gravitationally driven circulation held in check by the turbulence during periods of high tides can be studied.

NUNES and LENNON (1987) describe the adjustment of the density field in Spencer Gulf during periods of low tidal flow and wind stirring. The distribution of σ_t in June 1983 shown in Fig. 12b shows evidence of a cyclonic (clockwise) gyre which is the expected effect of the Earth's rotation on the gravitational circulation. Fig. 13 shows transects across the three sections shown in Fig. 12b. Pronounced frontal features are found on both the top and the bottom. The timescale t_c for frontogenesis given by (16), when applied to Spencer Gulf with $\alpha_1 = 2\alpha_2 = 1 \times 10^{-7} \text{ m}^{-1}$, is approximately 1.5 h. Thus frontogenesis is expected to occur, since the density contours adjust under gravity for several days.

Calculations of the effects of rotation with angular velocity $\frac{1}{2}f$ on the adjustment of a fluid with a uniform horizontal density gradient show the flow is turned in about one inertial period so that it is in approximate geostrophic balance with the density field. The tilting of the isopycnals is arrested at a finite angle $\theta = \tan^{-1}\{ga/f^2\}$ to the vertical. For Spencer Gulf the predicted value of θ is 89° , in agreement with the observed average slope of the isopycnals.

Columbia River Estuary, U.S.A.

In their general discussion of estuary classification JAY and SMITH (1988) present some interesting data on the Columbia River Estuary. In particular they show that during periods of spring tides the estuary is well mixed but during neaps a two-layer stratification with strong frontal features is observed (see their Figs 1 and 2). JAY and SMITH (1988) discuss the transition in terms of an internal Froude number characterization implying that the mixing is a result of shear instability on an interface. Shear instability leads to a thickening of the interface and some additional form of turbulence is required to produce vertical mixing. On the basis of our present experiments we suggest that the additional source of turbulence is that generated by stresses on the bottom of the estuary.

The restratification during neaps is consistent with the baroclinic circulation observed at low turbulence levels in our experiments. The horizontal density gradient is approximately piecewise linear with $\alpha_1 = 3\alpha_2 = 3 \times 10^{-7} \text{ m}^{-1}$. The timescale for frontogenesis is 0.8 h and so fronts can be expected to form at low tidal stirring. The form of the

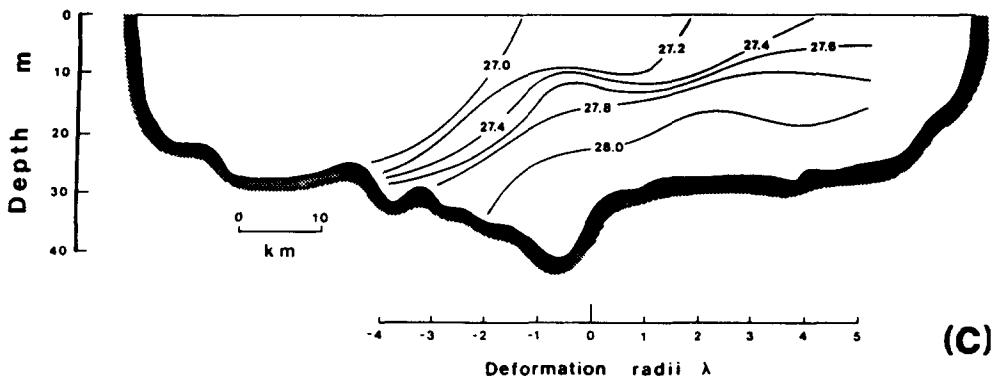
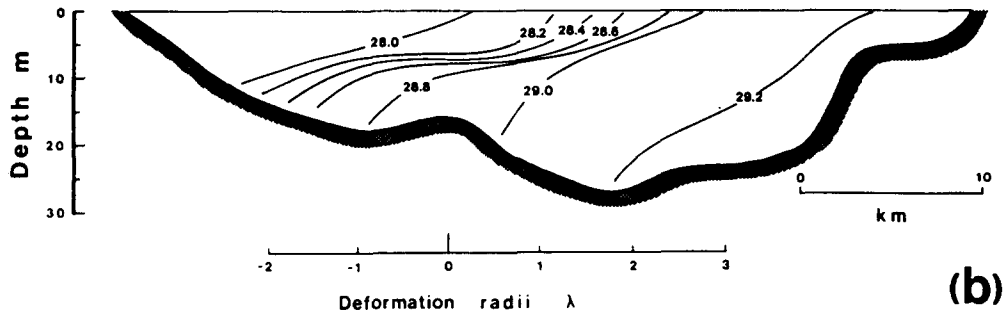
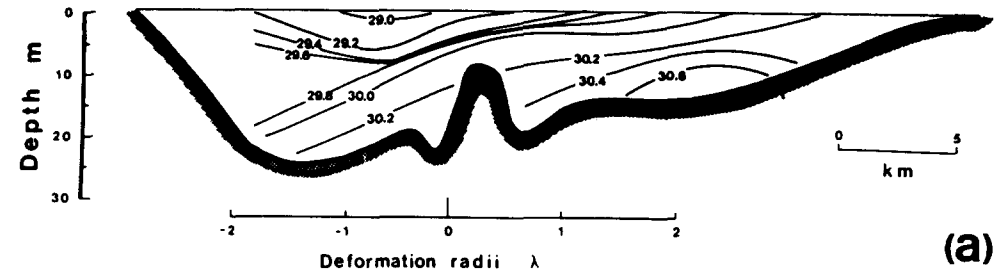


Fig. 13. Vertical section of $\sigma_t(\text{kg m}^{-3})$ at the three sections shown in Fig. 12.

horizontal stratification is such that $\rho_x < 0$ and $\rho_{xx} < 0$ where x is measured up-estuary from the mouth. Consequently a front is expected to occur at the surface and propagate towards the sea (SIMPSON and LINDEN 1988). These features are visible at the end of both the flood and the ebb tide at neaps (see JAY and SMITH, 1988; their Fig. 2). At the end of the flood there is also a bottom front, presumably caused by the intruding salt water.

6. CONCLUSIONS

In this paper we have discussed the effects of modulations in the level of environmental turbulence on the circulation produced in a fluid with a horizontal variation in density. A series of laboratory experiments have been carried out in which the horizontal flux of density has been measured and the effective longitudinal dispersion coefficient K has been calculated. We observe that the magnitude of the dispersion coefficient increases with the horizontal density gradient and with the period of the turbulence modulation. Both of these increases are due to the baroclinic circulation produced by the horizontal density gradient. Most notable is the dramatic increase in the transport of density in periods of low turbulence level when the baroclinic circulation is most effective.

We have made comparisons with oceanographic situations in which significant variations in the turbulence level are found. Our results suggest that strong baroclinic effects occur and that they explain many features of the observations. In the case of Spencer Gulf where the turbulence level is significantly reduced over several days the effect of the Earth's rotation is important. Frontogenesis is also observed in agreement with extrapolations from earlier laboratory experiments (SIMPSON and LINDEN, 1988).

In Liverpool Bay the situation appears to be more complex. The turbulence level modulates with the tidal flow and so is, presumably, approximately sinusoidal. Our experiments, on the other hand, have a square wave modulation. This simplification is probably quite satisfactory on the ebb tide when the vertical stratification is developed, since the stratification will reduce the mixing produced by the turbulence. On the flood, however, the square wave modulation is rather a poor approximation to the tidal response. The gradual reduction in the turbulence level may be one reason why a marked front is not observed in Liverpool Bay. Residual flows are observed to be parallel to the front (PRANDLE and RYDER, 1985) suggesting that Coriolis forces are important. It may also be the case in these shallow situations that the gravity driven flow is limited by friction and not by inertia as in the laboratory. These aspects deserve further study.

The comparison with the estuarine situation in the Columbia River Estuary also shows that a number of the features of the vertical stratification and its variation in time are consistent with the laboratory experiments.

In this paper we have emphasized the time-dependent effect produced by a tidal flow. The results show that it can be misleading to consider tidally averaged quantities in these situations, and much of the physics is excluded when variations during a tidal cycle are excluded.

Acknowledgements—We are grateful to Drs J. Matthews, J. Brown, R. Nunes and Profs J. H. Simpson and G. W. Lennon for allowing us to quote their data. This work was supported by the Natural Environment Research Council.

REFERENCES

- BURT W. V., S. NESHYBA and C. L. TRUMP (1986) Rapid alternating vertical temperature gradients in the East China Sea. *Continental Shelf Research*, **6**, 449–458.
- CZITROM S. P. R. (1986) The effect of river discharge on the residual circulation in the Eastern Irish Sea. *Continental Shelf Research*, **6**, 475–486.
- HANSEN D. M. and M. RATTRAY (1966) New dimensions in estuary classification. *Limnology and Oceanography*, **11**, 319–326.
- HOPFINGER E. J. and P. F. LINDEN (1982) Formation of thermoclines in zero-mean-shear turbulence subjected to a stabilizing buoyancy flux. *Journal of Fluid Mechanics*, **114**, 157–173.
- JAY D. A. and J. D. SMITH (1988) Residual circulation and classification of shallow, stratified estuaries. In: *Physical processes in estuaries*, J. DRONKERS and W. VAN LEUSSEN, editors, Springer-Verlag, Heidelberg (in press).
- LINDEN P. F. (1979) Mixing in stratified fluids. *Geophysical and Astrophysical Fluid Dynamics*, **13**, 3–23.
- LINDEN P. F. and J. E. SIMPSON (1986) Gravity-driven flows in a turbulent fluid. *Journal of Fluid Mechanics*, **172**, 481–497.
- LODER J. W. and D. A. GREENBERG (1986) Predicted positions of tidal fronts in the Gulf of Maine region. *Continental Shelf Research*, **6**, 397–414.
- NUNES R. A. and G. W. LENNON (1987) Episodic stratification and gravity currents in a marine environment of modulated turbulence. *Journal of Geophysical Research* (in press).
- PHILLIPS O. M. (1966) On turbulent convection currents and the circulation of the deep sea. *Deep-Sea Research*, **13**, 1149–1160.
- PRANDLE D. and D. K. RYDER (1985) Measurements of surface currents in Liverpool Bay by high frequency radar. *Nature*, **315**, 128–131.
- SIMPSON H. B. (1955) Some effects of upland discharge on estuarine hydraulics. *Proceedings of the American Society Civil Engineering*, **81**, No. 792.
- SIMPSON J. E. and P. F. LINDEN (1988) Frontogenesis in a fluid with horizontal density gradients. *Journal of Fluid Mechanics* (submitted).
- SIMPSON J. H. and J. R. HUNTER (1974) Fronts in the Irish Sea. *Nature*, **250**, 404–406.
- SIMPSON J. H., J. BROWN, J. M. MATTHEWS and G. ALLEN (1988) Tidal straining, density currents and stirring in the control of estuarine stratification. Proceedings of the Estuarine Research Federation Conference, New Orleans, October 1987. To be published in *Estuaries*.